

# Simultaneous Time- and Frequency-Domain Extrapolation

Raviraj S. Adve, *Member, IEEE*, and Tapan K. Sarkar, *Fellow, IEEE*

**Abstract**—In this paper, given the early-time response and the low-frequency response of a causal system, we simultaneously extrapolate them in the time and frequency domains. The approach is iterative and is based on a simple discrete Fourier transform. Simultaneous extrapolation in time and frequency domains is further enhanced by using the matrix pencil technique in the time domain and the Cauchy method in the frequency domain. The results are further enhanced through the Hilbert transform, hence enforcing the physical constraints of the system and thereby guaranteeing a causal extrapolation in time. It is, therefore, possible to generate information over a larger domain from limited data. It is important to note that through this extrapolation, no new information is created. The early-time and low-frequency data are complementary and contain all the desired information. The key is to extract this information in an efficient and accurate manner.

**Index Terms**—Extrapolation, frequency-domain analysis, time-domain analysis.

## I. INTRODUCTION

IN most of computational electromagnetics, the solution technique assumes a time-harmonic behavior for all field quantities. This implies that the solution is in the frequency domain. The principal reason for this has been that the frequency-domain formulations are more tractable analytically. Time-domain solutions are then found using an inverse Fourier transform.

Frequency-domain formulations use either the integral equation (IE) approach or the differential equation (DE) approach. In using an IE formulation, such as the method of moments (MoM), the spatial sampling has to be carried out in one spatial dimension less than the number of dimensions possessed by the problem. However, frequency-domain codes usually cannot efficiently handle multiple inhomogeneous media. Further, the matrix involved in the solution is full. DE formulations, like the finite-element method can treat medium inhomogeneities and nonlinearities in a more straightforward manner. However, the spatial sampling has to be carried out in as many spatial dimensions as possessed by the problem. Also, DE techniques are difficult to use in the case of unbounded regions [1].

The drawback to frequency-domain formulations is that the analysis program has to be executed for each frequency

Manuscript received October 2, 1995; revised December 2, 1997.

R. S. Adve is with Research Associates for Defense Conversion, Marcy, NY 13403 USA.

T. K. Sarkar is with the Department of Electrical Engineering and Computer Science, Syracuse University, Syracuse, NY 13244 USA.

Publisher Item Identifier S 0018-926X(98)02756-2.

of interest. Hence, a broad-band analysis can be very time consuming. Particularly when the frequency becomes high one needs to solve a large matrix equation, which takes an enormous amount of computer resources. Also, as the frequency of interest increases, the time required for analysis at each frequency point also increases.

With the increasing speed and memory of digital computers, many scattering problems are being performed in the time domain. There are four basic reasons for time domain modeling [2]. In certain electromagnetic problems, a time-domain formulation requires fewer arithmetic operations. Second, in seeking broad-band information, the time-domain model is intrinsically a better choice. The transient response obtained is limited only by the bandwidth of the excitation and the spatial discretization.

Another advantage of time-domain modeling is that problems involving nonlinear media can usually be modeled easily in the time domain. This advantage holds true for time-varying media. Handling nonlinear media and time-varying media can be extremely difficult in the frequency domain. The other reason for using time-domain analysis is that gating can be used to eliminate unwanted reflections.

A time-domain formulation using integral equations usually results in the method of marching on time (MOT). Here, the value of an unknown at a given time  $t_1$  is dependent on the excitation at  $t_1$  and the values of all the unknowns for  $t < t_1$ . By properly choosing a time step, an explicit solution for the unknowns can be obtained. However, MOT algorithms suffer from some serious defects. One main disadvantage is the persistent presence of late-time high-frequency oscillations. These usually unstable oscillations occur even when the time step is chosen such that the Courant stability condition is satisfied [3]. Many different approaches have been suggested to overcome these instabilities [4]–[6]. However, the stability problems have not been eliminated.

Time-domain formulations using DE's begin with the time-dependent Maxwell curl equations. These formulations usually require a “numerically gentle” turning on of the excitation. Hence, finding an impulse response is impossible from a time-domain DE code. A very popular time domain formulation is the finite-difference time-domain (FDTD); here, the differential operators are approximated by finite differences. However, here, too, the time variation is obtained through a time-stepping procedure. In addition, some sort of absorbing boundary conditions need to be imposed to terminate the spatial discretization at a finite distance from the scatterer, i.e., the spatial discretization is not allowed to extend to infinity.

In summary, modern-day computer programs can easily analyze an electromagnetic system in the low-frequency and early-time regions. In the low-frequency region, the analysis can be speedily performed with a few unknowns. In the early-time region, instabilities such as the late-time oscillations have not set in. For DE programs, an absorbing boundary condition is not necessary. Also, since the execution time of a MOT program is directly proportional to the analysis time period, the early time-domain analysis is not very time consuming.

These drawbacks in current methods create a need for a tool that can use information from both the time and frequency domains and yield broad-band frequency information and stable late-time information. The basic philosophy is as follows: consider that we require wide-band information about certain parameters both in the time and in the frequency domain. We utilize a frequency-domain technique such that the IE for the finite-element method (FEM) to generate information about the parameter from a low frequency  $f_1$  (close to dc—zero frequency) to some frequency  $f_2$ —this problem may be tractable for the computer at hand. Next, we use a time-domain code like the time-domain IE or FDTD or FEM-TD to generate information about the same parameter for the same excitation from time  $t = 0$  to  $t = T$ . As long as  $Tf_2 > 1$  and  $f_1 \simeq 0$ , we have all the necessary information desired from the partial solutions in time and frequency domains. The key is to find a method to extract this information. In this paper, a solution methodology is outlined.

It is important to point out that the simultaneous extrapolation in time and frequency domains tacitly assumes a bandlimited system. For example, when solving a frequency-domain problem, a spatial discretization of the scatterer by elements whose dimensions are of the order of a tenth of a wavelength in the medium of interest is used. In the time domain, the excitation is considered to be effectively bandlimited. The highest frequency up to which a solution can be accurately obtained is limited, again for time-domain problems, by the spatial discretization of the structure. Typically, as in the frequency domain, this highest frequency is such that the spatial discretization is of the order of a tenth of the wavelength.

In [7], Pereira-Filho and Sarkar present the matrix-pencil approach for extrapolating the time-domain data without requiring any frequency-domain information. This technique works very well if adequate time-domain data is available [8]. However, it suffers from one restriction. In the matrix-pencil approach, the required information is the free response of the system, i.e., the system response after the excitation has died down. In our current approach, no such restriction applies.

## II. EXTRAPOLATION BASED ON THE DISCRETE FOURIER TRANSFORM

Consider a function  $y(t)$  that represents the current as a function of time at a particular position on a scatterer. This current is the transient response to some known excitation. The associated frequency-domain response is represented by  $Y(j2\pi f)$ . The frequency and time domains are related through

the Fourier transform

$$Y(j2\pi f) = \int_0^\infty y(t)e^{-j2\pi f t} dt. \quad (1)$$

The Fourier integral starts at zero because the time domain response is causal, i.e.,  $y(t) = 0$ ,  $t < 0$ . As a result of using an integral-equation frequency-domain code we have samples of  $Y(j2\pi f)$  at  $f = i\Delta f$ ,  $i = 0, \dots, N_f - 1$ . On using a time-domain code based on MOT program we have samples of  $y(t)$  at  $t = k\Delta t$ ,  $k = 0, \dots, N_t - 1$ . Using this information, we want to find  $Y(2\pi f)$  up to  $F = M_f \Delta f$  and  $y(t)$  up to  $T = M_t \Delta t$ . Since we only have samples of  $Y(2\pi f)$  and  $y(t)$  at discrete points in  $t$  and  $f$ , instead of using the Fourier transform as defined in (1), we use the discrete Fourier transform pair [9].

$$Y_k \simeq \sum_{i=0}^{M_t-1} y_i e^{-j2\pi k \Delta f i \Delta t} \Delta t \quad (2)$$

$$y_i \simeq \sum_{k=0}^{M_f-1} Y_k e^{j2\pi k \Delta f i \Delta t} \Delta f \quad (3)$$

where,  $Y_k = Y(j2\pi k \Delta f)$  and  $y_i = y(i\Delta t)$ . To minimize the effects of discretization [10], the record length ( $M_f$  and  $M_t$ ) should be large.

In the simplest form, the proposed extrapolation procedure is as follows.

- 1) Pad the available time domain data ( $y_i$ ,  $i = 0, \dots, N_t - 1$ ) with zeros to create a sequence of length  $M_t$  such that  $M_t > 2N_t$ .
- 2) Perform a  $M_t$  point DFT on this sequence as defined by (2); define the resulting sequence to be  $Y'(k)$ ,  $k = 0, \dots, M_f - 1$ .
- 3) Replace the first  $N_f$  samples in  $Y'(k)$  with the known frequency-domain data  $Y_k$ ,  $k = 0, \dots, N_f - 1$ ; define the resulting sequence to be  $Y_{\text{new}}(k)$ .
- 4) Perform a  $M_f$  point inverse discrete Fourier transform (DFT) (IDFT) on  $Y_{\text{new}}(k)$  as defined by (3); define the resulting sequence to be  $y'(i)$ ,  $i = 0, \dots, M_t - 1$ .
- 5) Replace the first  $N_t$  samples in  $y'(i)$  with the known time-domain data  $y_i$ ,  $i = 0, \dots, N_t - 1$ ; define the resulting sequence to be  $y_{\text{new}}(i)$ .
- 6) Subsequent processing is an iteration on Steps 2–5.

The extrapolated data is in  $Y_{\text{new}}(k)$ ,  $k = 0, \dots, M_f - 1$  and  $y_{\text{new}}(i)$ ,  $i = 0, \dots, M_t - 1$ .

The DFT is used over the quicker fast Fourier transform (FFT) because in a DFT there are no restrictions on the frequency step or the number of samples. In a FFT  $M_t \Delta t \Delta f = M_f \Delta t \Delta f = 1$ . However, there are some hidden problems with the above extrapolation procedure. As explained by Brigham [10], a “discontinuity” in the data sequence produces the discrete equivalent of the Gibbs phenomenon. In our case, such a discontinuity arises because of the replacing the known data  $Y_k$  into  $Y'(k)$  [Step 3] and replacing  $y_i$  into  $y'(i)$  [Step 5]. As explained in (2) and (3), even if the entire data sequences  $y(i)$ ,  $i = 0, \dots, M_t - 1$  and  $Y_k$ ,  $k = 0, \dots, M_f - 1$  were known perfectly, the DFT and IDFT produce only approximations to the real  $Y_k$  and  $y_i$ . Hence, when replacing the known data into these sequences, a discontinuity arises at

sample number  $N_t$  in  $y_{\text{new}}(i)$  and at sample number  $N_f$  in  $Y_{\text{new}}(k)$ .

Brigham suggests the use of windows to minimize this discontinuity. Harris [11] details the use of many windows. However, the use of a window reduces resolution of the DFT and IDFT. Nonuniform sampling can be utilized through the use of the DFT technique described in [12]. However, here, the high-frequency Gibbs phenomenon is reduced, but not eliminated. Hence, in this work we smooth over the discontinuity to eliminate the Gibbs phenomenon. In the frequency domain, we use the Hilbert transform [13], [14] and the Cauchy method [15] to smooth over the discontinuity. In the time domain, data is smoothed using the matrix pencil technique [7], [8].

#### A. The Hilbert Transform

To maximize the use of the given information and to smooth the data in the frequency domain, we use a method based on the Hilbert transform as described in [13]. The method is an iterative technique to extrapolate/interpolate frequency-domain data relying on the fact that the underlying time-domain data is causal. It then uses the property that if the underlying time-domain data is causal, the real and imaginary parts of the frequency-domain response have to be related through the Hilbert transform [9]. The details of the method can be found in [13], [14].

In this application, the given information is the first  $N_f$  frequency-domain samples. Using this and the  $Y'(k)$  found in Step 2) as the initial guess, the output is a smoother frequency response.

#### B. The Cauchy Method

The Cauchy method provides an approximation for a function by a ratio of two polynomials if the function values and its derivatives are available at some, not necessarily equispaced, points. The frequency response is modeled as

$$Y(s) \simeq \frac{A(s)}{B(s)} = \frac{\sum_{k=0}^P a_k s^k}{\sum_{k=0}^Q b_k s^k}, \quad s = k\Delta f. \quad (4)$$

Given  $Y_{\text{new}}(k)$  at samples  $k = 0, \dots, M_f - 1$ , the problem reduces to finding the order of the polynomials and the coefficients that define them. The algorithm converts the above equation to a matrix equation to estimate the polynomial orders and the coefficients. In practice, the polynomial orders are not large (usually  $< 10$ ) and so the information required to estimate the orders and the coefficients is not as much as is available. Indeed, unnecessarily over determining the system of equations leads to numerical errors. The details of the Cauchy method are available in [15]–[17].

To smooth the data around  $k = N_f$ , we use the  $\frac{N_f}{2}$  samples before sample number  $N_f$  and  $\frac{N_f}{2}$  samples starting from sample number  $N_f + \frac{N_f}{2}$ . Using this information and the Cauchy method, we estimate the samples from number  $N_f + 1$  to  $N_f + \frac{N_f}{2} - 1$ . This results in a smoother data set.

#### C. The Matrix Pencil

The matrix pencil method models the time-domain sequence as a sum of complex exponentials

$$y(t) = \sum_{j=1}^M R_j e^{s_j t}. \quad (5)$$

Such a model is valid because the scatterer can be treated as a linear time-invariant (LTI) system. Given the  $M_t$  samples in  $y'(i)$ , the problem reduces to estimating  $M$ ,  $R_j$  and  $s_j$ . Once these parameters are found,  $y(t)$  can be evaluated at the desired time points  $t = i\Delta t$ . In the matrix pencil approach too the problem is formulated as a matrix equation. Hence, here too, unnecessarily over determining the system of equations leads to numerical errors. The details of the matrix pencil algorithm and a copy of the associated program can be found in [7].

We use the  $\frac{N_t}{2}$  samples just before sample number  $N_t$  to get one estimate of the response at the sample numbers  $N_t + 1$  to  $N_t + \frac{N_t}{10}$ . Another estimate is found by using the  $\frac{N_t}{2}$  samples starting at number  $N_t + \frac{N_t}{10} + 1$  in a reverse order. A moving average of these two estimates gives us a smooth data set for the time domain sequence.

#### D. The Extrapolation Procedure

The Hilbert transform, the Cauchy method and the matrix pencil method each have a strong physical basis. Therefore, using these three signal processing tools results in minimizing the errors providing a smooth extrapolation. This is crucial because the technique is iterative and the errors would accumulate leading to severe instabilities.

On using these tools, the updated iteration procedure is as follows.

- 1) Pad the available time-domain data with estimates of the samples using the matrix pencil to create a sequence of length  $M_t$ .
- 2) Perform a  $M_t$  point DFT on this sequence; define the resulting sequence to be  $Y'(k)$ ,  $k = 0, \dots, M_f - 1$ .
- 3) Use the Hilbert transform to smooth the data and get a better estimate of the frequency response.
- 4) Replace the first  $N_f$  samples in  $Y'(k)$  with the known frequency domain data  $Y_k$ ,  $k = 0, \dots, N_f - 1$ ; define the resulting sequence to be  $Y_{\text{new}}(k)$ .
- 5) Use the Cauchy method to smooth the data around sample number  $N_f$ .
- 6) Perform a  $M_f$  point IDFT on  $Y_{\text{new}}(k)$ ; define the resulting sequence to be  $y'(i)$ ,  $i = 0, \dots, M_t - 1$ .
- 7) Replace the first  $N_t$  samples in  $y'(i)$  with the known time-domain data  $y_i$ ,  $i = 0, \dots, N_t - 1$ ; define the resulting sequence to be  $y_{\text{new}}(i)$ .
- 8) Smooth the time-domain data around sample number  $N_t$  using the matrix pencil.
- 9) Subsequent processing is an iteration on Steps 2)–8).

### III. NUMERICAL EXAMPLES

To validate this iterative technique and to evaluate its usefulness, the above algorithm is tested on five examples. A program to evaluate the currents on an arbitrary shaped closed

or open body using the electric field integral equation (EFIE) and triangular patching is used [18]. The rational is that we use the EFIE in both the time [3] and in frequency domains [18], using the same surface patching scheme for both domains. This approach eliminates some of the effects of discretization from this study. The triangular patching approximates the surface of the scatterer with a set of adjacent triangles. Fig. 1 shows an example of the triangulation scheme used. The figure shows a disk being approximated by 128 triangles and 208 edges. The current perpendicular to each nonboundary edge is an unknown. The frequency-domain data has been generated using the program described in [18]. The spatial discretization limits the highest frequency to which the solution can be accurately computed.

Although the program can be used with an arbitrary excitation, we use a linearly polarized plane wave with a Gaussian profile in time. The excitation has the form

$$\mathbf{E}^{\text{inc}} = \mathbf{u}_i E_0 e^{-\frac{\gamma^2}{2}} \quad (6)$$

where

$$\gamma = \frac{(t - t_0 - \mathbf{r} \cdot \mathbf{k})}{\sigma} \quad (7)$$

- $\mathbf{u}_i$  the unit vector that defines the polarization of the incoming plane wave;
- $E_0$  the amplitude of the incoming wave;
- $\sigma$  controls the width of the pulse;
- $t_0$  a delay and is used so the pulse rises smoothly from zero for time  $t < 0$  to its value at time  $t$ ;
- $\mathbf{r}$  the position of an arbitrary point in space;
- $\mathbf{k}$  the unit wave vector defining the direction of arrival of the incident pulse.

The spectrum of this Gaussian plane wave is given by

$$F(j\omega) = \sqrt{2\pi\sigma} e^{-\left(\frac{(\omega\sigma)^2}{2} + j\omega t_0\right)}, \quad \omega = 2\pi f.$$

To obtain the response to the above Gaussian plane wave, the frequency response of the system is multiplied by the Gaussian spectrum.

The bodies chosen are a plate, a disk, a sphere, a cube, and a cone-hemisphere combination. All bodies are assumed to be perfectly conducting. In all computations  $E_0$  is chosen to be 377 V/m. The program uses five iterations and the smoothing procedure based on the Hilbert transform uses twenty iterations. To yield an explicit solution for the unknown currents, the time step ( $\Delta t$ ) is determined by the spatial discretization used in each example. The frequency step ( $\Delta f$ ) is 2 MHz.

In all the examples, the extrapolated time-domain response is compared to the output of the MOT program. In the figures, the extrapolated time response is labeled “reconstructed time response,” while the output of the MOT program is labeled “response from MOT.” The extrapolated frequency-domain response is compared to the frequency response obtained from the MoM program. The figures compare magnitudes of the frequency-domain responses. The extrapolated response is labeled “reconstructed response” while the output of the MoM program is labeled “response from MoM.”

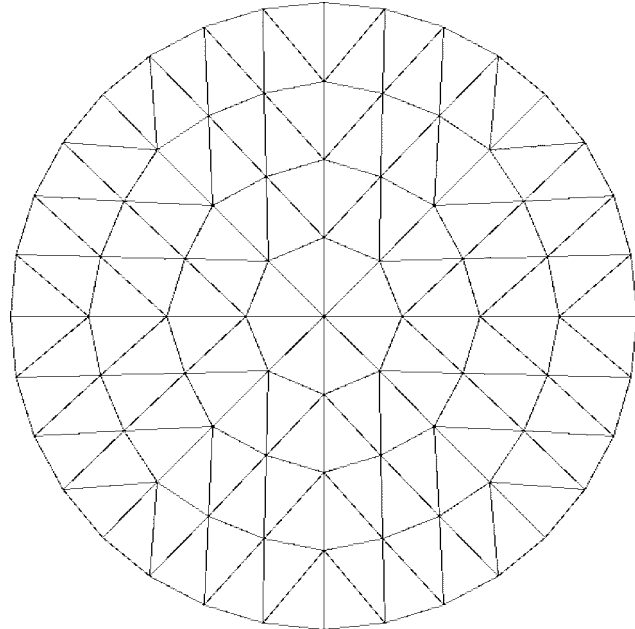


Fig. 1. Triangle patching of a disk.

**Example 1—Square Plate:** The first example we present is a square plate of zero thickness and side 1 m, centered at the origin. The plate is located in the  $xy$  plane. Eight divisions are made in the  $x$  direction and nine in the  $y$  direction. By joining the diagonals of each resulting rectangle, 144 triangular patches with 199 unknowns are obtained. This division scheme allows us to evaluate the current at the center of the plate. The excitation arrives from the direction  $\theta = 0$ ,  $\phi = 0$ , i.e., along the negative  $z$  direction.  $\mathbf{u}_i$  is along the  $x$  axis. In this example,  $\sigma = 2$  ns and  $t_0 = 10$  ns. The time step used in the MOT program is 92.59 ps.

In this example, the MOT program evaluates the current at the center for the first 1500 time steps (from  $t = 0$  to  $t = 0.138 \mu\text{s}$ ). The MoM program evaluated the frequency response at 501 samples (from  $f = 0$  to  $f = 1$  GHz). The first 233 time samples (upto  $t = 21.48$  ns) and the first 37 frequency samples (up to  $f = 72$  MHz) have been used as input to the computer program. In this case,  $f_2 T = 1.55$ . Using this data, the program extrapolated the time-domain data up to 1500 samples ( $M_t = 1500$ ) and the frequency domain data upto 501 samples ( $M_f = 501$ ). The results of the extrapolation in the time domain can be seen in Fig. 2. As can be seen the reconstruction is indistinguishable from the output of the MOT program.

The frequency response of the system is shown in Fig. 3. The extrapolation is shown up to 500 MHz (the first 251 samples) since for frequencies higher than 500 MHz the response is very close to zero. Fig. 3 shows the comparison of the magnitudes of the frequency responses. The reconstruction is nearly perfect and is visually indistinguishable from the results of the MoM program.

**Example 2—Disk:** The next example is a disk of zero thickness, as shown in Fig. 1. The disk lies in the  $xy$  plane and is centered at the origin. It has a radius of 0.3 m. The triangulation uses 128 triangles resulting in 208 edges. 32 of

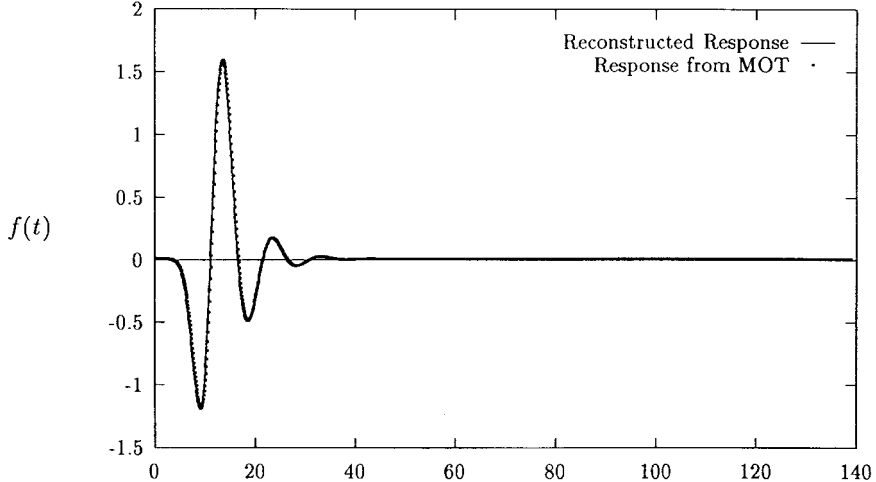


Fig. 2. Time-domain response of the plate.

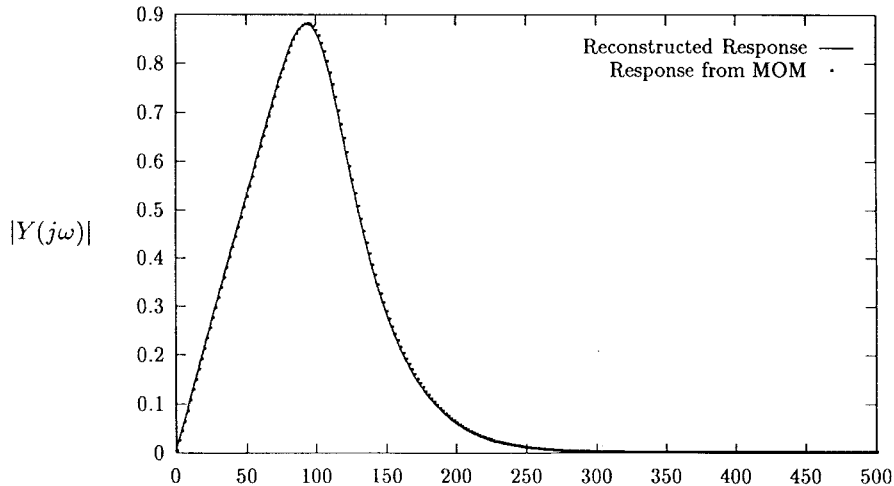


Fig. 3. Frequency-domain response of the plate.

the edges are boundary edges yielding 176 unknowns. The excitation arrives from  $\theta = 0, \phi = 0$ , i.e., along the negative  $z$  direction.  $\mathbf{u}_i$  is along the  $x$  axis. Here,  $\sigma = 1$  ns and  $t_0 = 10$  ns. The time step used is 47.76 ps.

In this example, the MOT program evaluated the current at the center for the first 1500 time steps (from  $t = 0$  to  $t = 71.59$  ns). The MoM evaluated the frequency response at 501 frequency points (from  $f = 0$  to  $f = 1$  GHz). The first 334 time samples (up to  $t = 15.90$  ns) and the first 95 frequency points (up to  $f = 188$  MHz) are used as input to the extrapolation program, i.e., for this example,  $f_2 T = 2.99$ . Using this data, the program extrapolated in the time domain up to 1500 samples and in the frequency upto 501 samples. The results of the time-domain extrapolation are shown in Fig. 4.

The frequency response of this system is shown in Fig. 5. The extrapolation is shown up to 600 MHz above which the response is very close to zero. Fig. 5 compares the magnitude of the reconstructed frequency response with the output of the MoM program. The agreement between the computed

responses and the reconstructed responses both in the time and frequency domains appears to be reasonable.

*Example 3—Sphere:* The next example is a sphere of radius 0.5 m. The sphere is centered at the origin. The “top” half of the sphere ( $\theta = 0$  to  $\theta = \frac{\pi}{2}$ ) has six divisions in the  $\theta$  direction. The first “ring” extends from  $\theta = 0$  to  $\theta = \frac{\pi}{16}$ . The other five rings are equispaced in  $\theta$  from  $\theta = \frac{\pi}{16}$  to  $\theta = \frac{\pi}{2}$ . Each ring, starting from the top has 6, 16, 20, 24, 28, and 32 triangular patches. The sphere is symmetric with respect to the  $xy$  plane. This scheme is chosen so all triangles as close to equilateral as possible. If the  $\phi$  direction were also divided uniformly, the triangles would be skewed. Also, this scheme allows us to evaluate the current at the point  $(-0.5, 0.0, 0.0)$ .

The excitation arrives from  $\theta = \frac{\pi}{2}, \phi = \pi$ , i.e., along the  $x$  direction.  $\mathbf{u}_i$  is along the  $z$  axis. In this example  $\sigma = 3$  ns and  $t_0 = 22$  ns. The time step used in the MOT program is 0.19943 ns.

The MOT program evaluated the current at the point  $(-0.5, 0.0, 0.0)$  for the first 500 time steps (from  $t = 0$  to  $t = 99.515$  ns). The MoM program evaluated the current for the first

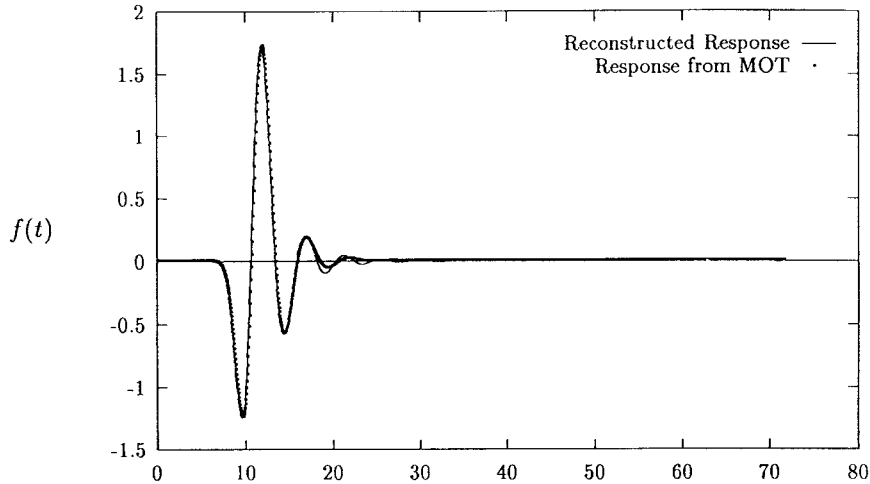


Fig. 4. Time-domain response of the disk.

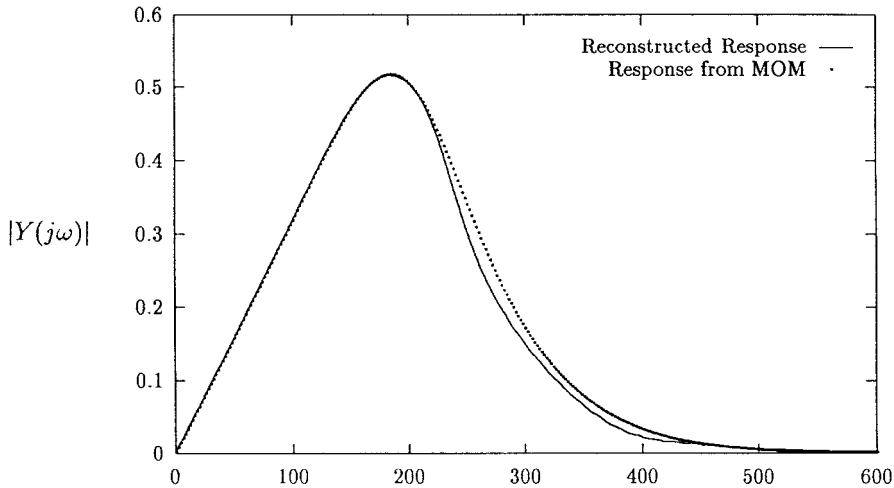


Fig. 5. Frequency-domain response of the disk.

501 frequency samples (up to  $f = 1$  GHz). The first 183 time samples (up to  $t = 36.29$  ns) and the first 37 frequency samples (up to  $f = 72$  MHz) are input to the program resulting in  $f_2 T = 2.61$ . Using this information, the extrapolation is carried out with  $M_t = 500$  and  $M_f = 501$ .

The results of the extrapolation in the time domain are shown in Fig. 6. As can be seen, even for only 500 time samples, the output of the MOT program is quite unstable and gives erroneous results. However, the extrapolated results are relatively stable. This is an advantage of this method. The late-time information is mainly obtained from the low-frequency data. This given data is stable and, hence, the late time information is stable. In using an integral equation MOT program, the late-time information is frequently unstable.

The frequency-domain extrapolation is shown in Fig. 7. The extrapolation is shown upto 300 MHz since above 300 MHz the response is close to zero. In Fig. 7 the magnitude of the extrapolated frequency response is compared to the response obtained from the MoM program. The agreement between the reconstructed response and the response obtained from the MoM is reasonable.

*Example 4—Cube:* The fourth example is a cube of side 1 m centered at the origin. The faces of the cube are lined along the three coordinate axes. The faces at  $x = 0.5$  m and  $x = -0.5$  m have five divisions in the  $y$  and  $z$  direction. All other faces have four divisions in one direction and five in the other. This allows us to find the current at the center of the top face. The excitation arrives from the direction  $\theta = 0$ ,  $\phi = 0$ , i.e., along the  $-z$  axis.  $\mathbf{u}_i$  is along the  $x$  axis. In this example,  $\sigma = 2.357$  ns and  $t_0 = 20$  ns. The time step chosen for the MOT program is 0.15713 ns.

The MOT program evaluated the current at the center of the top face for the first 500 time steps (from  $t = 0$  to  $t = 78.41$  ns). The MoM program evaluated the frequency response at 501 samples (from  $f = 0$  to  $f = 1$  GHz). The first 193 time samples (up to  $t = 30.17$  ns) and the first 49 frequency points (up to  $f = 96$  MHz) were used as the given data. For this example,  $f_2 T = 2.9$ . Using this information, the time and frequency domains were extrapolated with parameters  $M_t = 500$  and  $M_f = 501$ . Fig. 8 shows the results of the time-domain extrapolation. Here, again, we see that while the MOT program has started to give unstable results, the extrapolated time-domain response is stable.

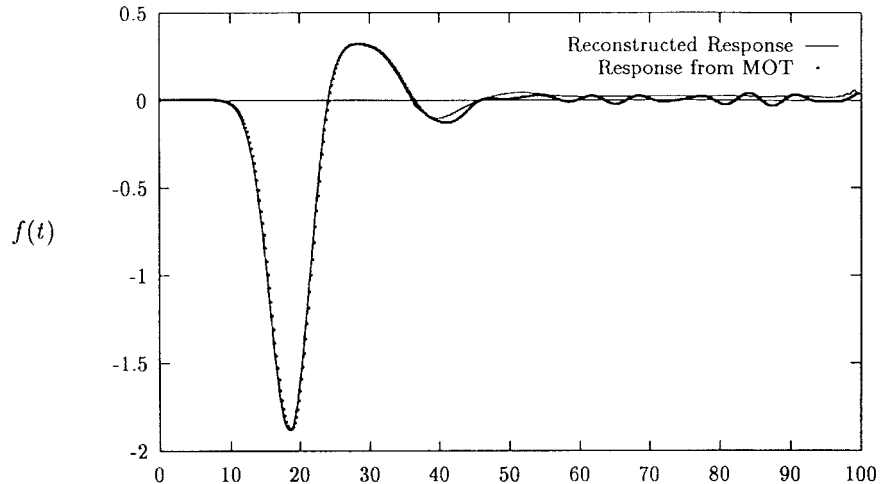


Fig. 6. Time-domain response of the sphere.

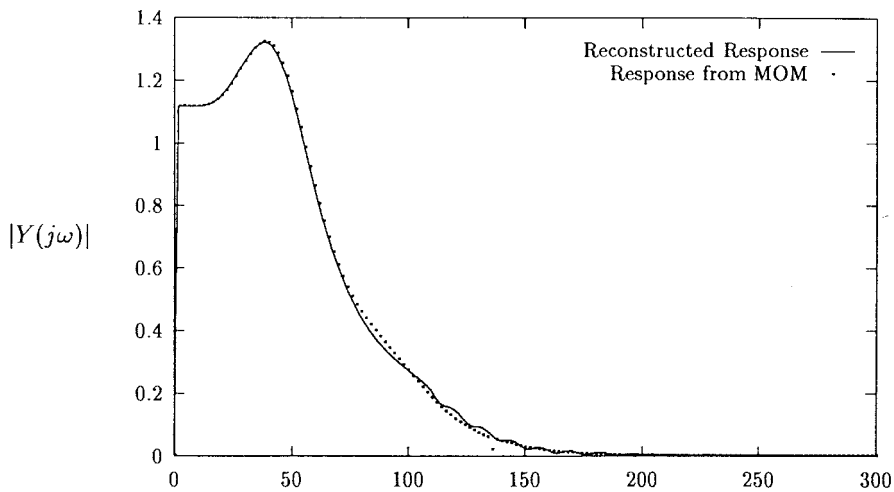


Fig. 7. Frequency-domain response of the sphere.

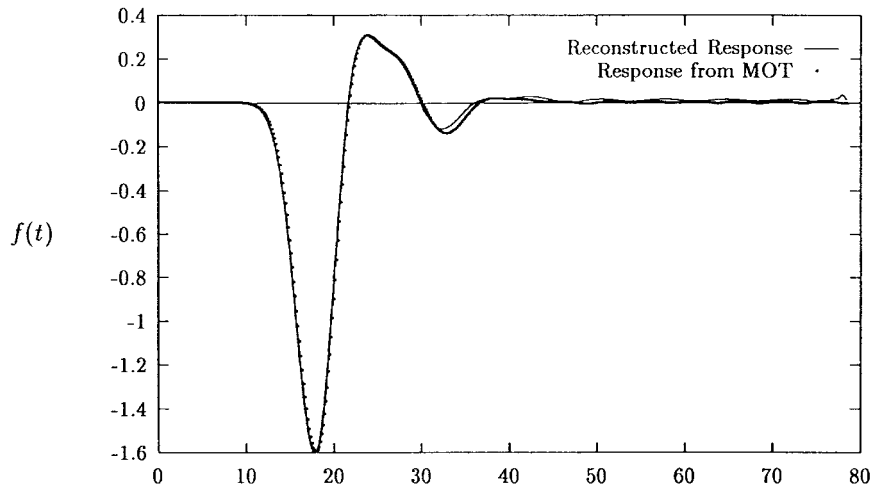


Fig. 8. Time-domain response of the cube.

The frequency response of this system, up to 300 MHz is shown in Fig. 9. The reconstructed response and the response obtained from the MoM are close.

*Example 5—Cone-Hemisphere:* The final example, we have chosen is a combination of a cone and a hemisphere. The hemisphere is attached to the base of the cone forming

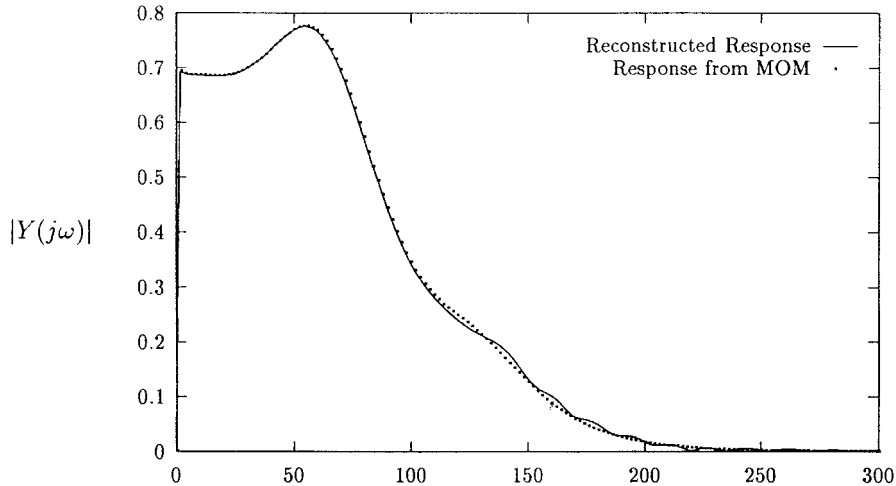


Fig. 9. Frequency-domain response of the cube.

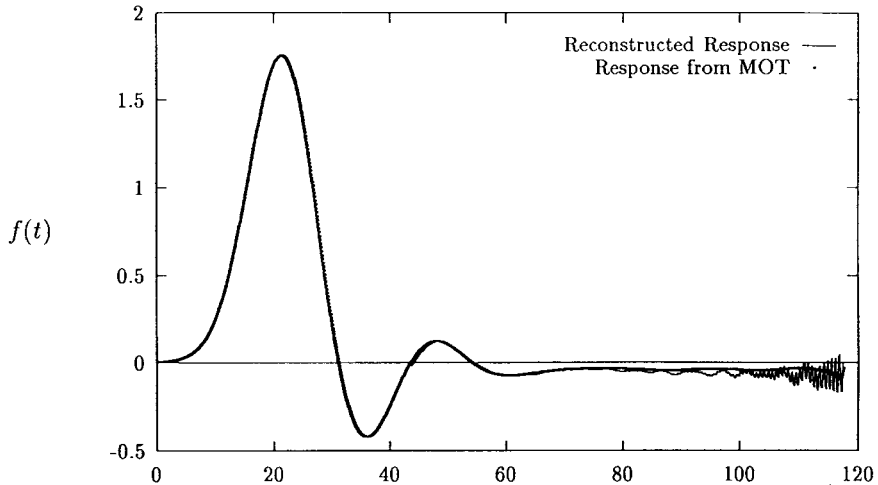


Fig. 10. Time-domain response of the cone hemisphere.

one compound three-dimensional object. The base of the cone and hemisphere is centered at the origin. The base of the cone and hemisphere have a radius of 1 m. The height of the cone is 2 m. The central axis of the combination lies on the  $z$  axis.

The triangular patch approximation for the cone has six divisions in the  $z$  direction. The planes defining the “rings” are at  $z = 2.0$ ,  $z = 1.75$ ,  $z = 1.4$ ,  $z = 1.05$ ,  $z = 0.7$ ,  $z = 0.35$ , and  $z = 0$ . Each ring, starting from the top has 7, 16, 20, 24, 28, and 32 triangles, respectively. The hemisphere has three divisions in the  $\theta$  direction. The “rings” extend from  $\theta = \pi$  to  $\theta = \frac{2\pi}{3}$ ,  $\theta = \frac{5\pi}{6}$  to  $\theta = \frac{2\pi}{3}$ , and  $\theta = \frac{2\pi}{3}$  to  $\theta = \frac{\pi}{2}$ . Each ring, starting from the bottom, has 13, 28, and 32 triangular patches, respectively. Such a triangulation scheme allows for the current at the point  $(-0.1, 0.0, 0.0)$  to be evaluated.

The excitation arrives from  $\theta = \frac{\pi}{2}$ ,  $\phi = \pi$ , i.e., along the  $x$  direction.  $\mathbf{u}_i$  is along the  $z$  axis. In this example,  $\sigma = 6$  ns and  $t_0 = 25$  ns. The time step used is 90.39 ps. The frequency step used is 2 MHz.

The MOT program evaluated the first 1300 time samples (from  $t = 0$  to  $t = 117.42$  ns). The MoM program evaluated the first 501 frequency samples (from  $f = 0$  to  $f = 1$  GHz). The first 482 time samples (upto  $t = 43.97$  ns) and the first 25 frequency samples (up to  $f = 48$  MHz) were used as input

to the time-frequency extrapolation program. This results in  $f_2 T = 2.11$ . Using this information the time-domain response was extrapolated to 1300 samples and the frequency domain to 501 samples. The results of the time-domain extrapolation are shown in Fig. 10. As seen the data from the MOT program (labeled “response from MOT”) is unstable for late times. However, the reconstructed time response continues to be stable.

The magnitude of the reconstructed frequency-domain response is compared with the magnitude of the frequency response obtained from the MoM. The agreement between the two responses is good.

#### IV. CONCLUSION

In this paper, we have presented a technique based on the Fourier transform for simultaneous extrapolation in the time and frequency domains. Because the required information is only the early-time response and the low-frequency response, the technique yields major savings in program execution time. Typically, for good reconstruction it appears that one needs a time-bandwidth product of the order of 1.5–3.0. However, this factor is dependent on the quality of the time and frequency-domain data. Since two smaller problems are solved, the computer resources required are modest. Even though the

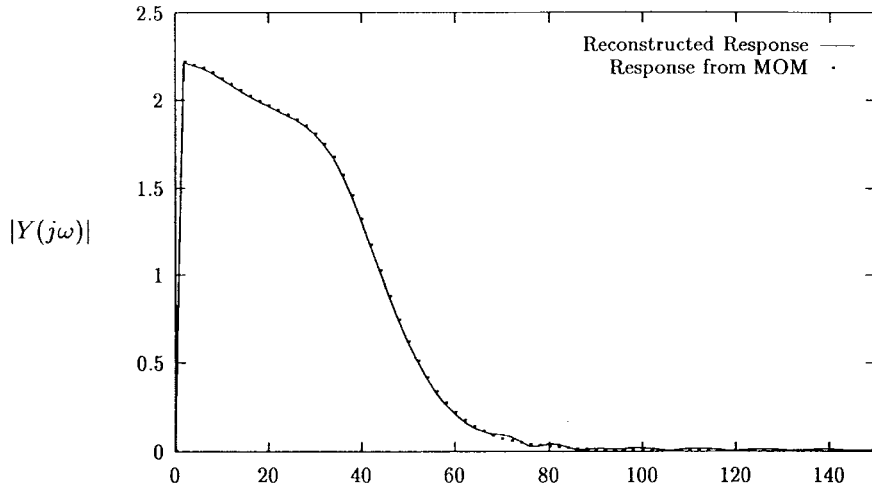


Fig. 11. Frequency response of the cone hemisphere.

starting information is obtained from techniques that have the potential to become unstable in late times, the extrapolation scheme does not exhibit such behavior.

It is important to note that the early time-domain data and low-frequency domain data are complementary. The extrapolation does not create any new information. The early-time data provides the missing high-frequency information and the low-frequency data provides the late-time information. The Hilbert and Fourier transforms are utilized to combine the complementary data and perform extrapolation.

As the Fourier transform, the Hilbert transform, the Cauchy and matrix-pencil methods are independent of the electromagnetic issues, the specific application from numerical electromagnetics is irrelevant. In this paper, we apply the extrapolation procedure to the problem of extrapolating the current on a scatterer being excited by a uniform plane wave.

To test the proposed technique, the algorithm has been tested on five different examples. The number of time-domain samples to be used by the extrapolation technique was chosen such that the response used extends a short time after the excitation has died down. The number of frequency samples used was chosen such that the first resonance is included. Currently, work is under way to generalize this case to more than one resonance. We have seen that the technique yields accurate extrapolated results over a wide dynamic range in both time and frequency domains. The examples presented have only one resonance in the frequency domain.

## REFERENCES

- [1] E. K. Miller, "A selective survey of computational electromagnetics," *IEEE Trans. Antennas Propagat.*, vol. 36, pp. 1281–1305, Sept. 1988.
- [2] ———, "Time domain modeling in electromagnetics," *J. Electromagn. Waves Appl.*, vol. 8, nos. 9/10, pp. 1125–1172, 1994.
- [3] D. A. Vechinski, "Direct time-domain analysis of arbitrarily shaped conducting or dielectric structures using patch modeling techniques," Ph.D. dissertation, Auburn University, Auburn, AL, 1992.
- [4] P. Rynne, "Instabilities in time marching methods for scattering problems," *Electromagn.*, vol. 4, pp. 129–144, 1986.
- [5] A. G. Tijhuis, "Toward a stable marching-on-in-time method for two dimensional transient electromagnetic scattering problems," *Radio, Sci.*, vol. 19, pp. 1311–1317, 1984.
- [6] P. D. Smith, "Instabilities in time-marching methods for scattering: Cause and rectification," *Electromagn.*, vol. 10, pp. 439–451, 1990.
- [7] O. M. Pereira-Filho and T. K. Sarkar, "Using the Matrix Pencil method to estimate the parameters of a sum of complex exponentials," *IEEE Antennas Propagat. Mag.*, vol. 37, pp. 48–55, 1995.
- [8] T. K. Sarkar, R. S. Adve, O. M. Pereira-Filho, and S. M. Rao, "Extrapolation of time domain responses from three dimensional objects utilizing the matrix pencil technique," *IEEE Trans. Antennas Propagat.*, vol. 45, pp. 147–156, Jan. 1997.
- [9] A. V. Oppenheim and R. W. Schafer, *Discrete-Time Signal Processing*. Englewood Cliffs, NJ: Prentice-Hall, 1989.
- [10] E. O. Brigham, *The Fast Fourier Transform*. Englewood Cliffs, NJ: Prentice-Hall, 1974.
- [11] F. J. Harris, "On the use of windows for harmonic analysis with the discrete Fourier transform," *Proc. IEEE*, vol. 66, pp. 51–83, 1978.
- [12] F. J. Sulkowski, "A program to calculate inverse Fourier transforms," Tech. Rep. AF 29(601)-7283, Dikewood Corp., Nov. 1966.
- [13] S. M. Narayana, S. M. Rao, R. S. Adve, T. K. Sarkar, V. Vannicola, M. Wicks, and S. A. Scott, "Interpolation/extrapolation of frequency responses using the Hilbert transform," *IEEE Trans. Microwave Theory Tech.*, vol. 44, pp. 1621–1627, Oct. 1996.
- [14] S. M. Narayana, T. K. Sarkar, R. S. Adve, M. Wicks, and V. Vannicola, "A comparison of two techniques for the interpolation/extrapolation of frequency responses," *Digital Signal Processing*, vol. 6, pp. 51–67, 1996.
- [15] R. S. Adve, T. K. Sarkar, S. M. Rao, E. K. Miller, and D. R. Pflug, "Application of the Cauchy method for extrapolating/interpolating narrowband system responses," *IEEE Trans. Microwave Theory Tech.*, vol. 45, pp. 837–845, May 1997.
- [16] R. S. Adve and T. K. Sarkar, "Generation of accurate broadband information from narrowband data using the Cauchy method," *Microwave Opt. Technol. Lett.*, vol. 6, pp. 569–573, 1993.
- [17] ———, "The effect of noise in the data on the Cauchy method," *Microwave Opt. Technol. Lett.*, vol. 7, pp. 424–427, Apr. 1994.
- [18] S. M. Rao, "Electromagnetic Scattering and radiation of arbitrarily shaped surfaces by triangular patch modeling," Ph.D. dissertation, Univ. Mississippi, University, MS, 1978.



**Raviraj S. Adve** (S'88–M'97) was born in Bombay, India. He received the B.Tech. degree in electrical engineering from Indian Institute of Technology, Bombay, in 1990, and the Ph.D. degree from Syracuse University, Syracuse, NY, in 1996.

He is currently working for Research Associates for Defense Conversion (RADC) Inc. under contract with the Air Force Research Laboratory at Rome, NY. His dissertation research investigated the effects of mutual coupling between the elements of adaptive antenna arrays on the performance of

space-time adaptive processing algorithms. His current research interests include the applications of numerical electromagnetic techniques to adaptive radar systems and wireless communications. He has also investigated the applications of signal processing techniques to numerical and experimental electromagnetics.



**Tapan K. Sarkar** (SM'69–M'76–SM'81–F'92) received the B.Tech. degree from the Indian Institute of Technology, Kharagpur, India, in 1969, the M.Sc.E. degree from the University of New Brunswick, Fredericton, Canada, in 1971, and the M.S. and Ph.D. degrees from Syracuse University, Syracuse, NY, in 1975.

From 1975 to 1976, he was with the TACO Division of the General Instruments Corporation, NY, and from 1976 to 1985 he was with the Rochester Institute of Technology, Rochester, NY.

He was a Research Fellow at the Gordon McKay Laboratory, Harvard University, Cambridge, MA from 1977 to 1978. He is now a Professor in the Department of Electrical and Computer Engineering, Syracuse University. His current research interests include numerical solutions of operator equations arising in electromagnetics and signal processing with application to system design. He has authored or coauthored more than 150 journal articles and conference papers and has written chapters in eight books.

Dr. Sarkar is a registered Professional Engineer in the State of New York. He received the Best Paper Award of the IEEE TRANSACTIONS ON ELECTROMAGNETIC COMPATIBILITY in 1979 and received one of the "Best Solution" Awards in May 1977 at the Rome Air Development Center (RADC) Spectral Estimation Workshop. He was an Associate Editor for feature articles of the *IEEE Antennas and Propagation Society Newsletter*. He was the Technical Program Chairman for the 1988 IEEE Antennas and Propagation Society International Symposium and URSI Radio Science Meeting. He was appointed United States Research Council Representative to many URSI General Assemblies. He is the Chairman of the Intercommission Working Group of International URSI on Time Domain Metrology. He is a member of Sigma Xi and International Union of Radio Science Commissions A and B.